



Palynofacies associated to hyperpycnite deposits of the Miocene, Cabo Viamonte Beds, Austral Basin, Argentina

Mirta E. Quattrocchio^{1,2} · Daniela E. Olivera^{1,2} · Marcelo A. Martínez^{1,2} · Juan J. Ponce³ · Noelia B. Carmona³

Received: 7 November 2017 / Accepted: 30 May 2018
© Springer-Verlag GmbH Germany, part of Springer Nature 2018

Abstract

The Miocene deposits in the Punta Basílica locality, southernmost Argentina, are included within the Cabo Viamonte Beds, Cabo Domingo Group, in the Austral foreland basin of Tierra del Fuego province. The prograding clinoform systems were accumulated during a weak compressional tectonic regime that allowed the development of a narrow shelf. Paleoenvironmental reconstructions suggest that these clinoforms comprise two dominant architectural elements, channel-levee and lobe complexes, formed mainly by density hyperpycnal currents in outer shelf to depositional slope environments. The transitional and recurrent (vertical and lateral) alternation between sedimentary structures without rheologic boundaries associated with the co-occurrence of plant remains (*Nothofagus*) are diagnostic criteria for the recognition of hyperpycnites. This type of density flow typically transports large volumes of sediment and organic matter from proximal to deep-marine settings. Four palynofacies types were recognized in a cluster analysis. In general, the palynofacies show predominance of spores and pollen grains, tissues, cuticles, and spongy to fibrous amorphous organic matter (plant and/or freshwater to brackish algae derived), which reflect different positions within the depositional system (e.g., levee-channel and lobe deposits). The co-occurrence of inshore (*Batiacasphaera* spp., *Lingulodinium* sp.) with relatively more oceanic (*Operculodinium centrocarpum*, *Spiniferites* spp.) dinoflagellates is a strong indication that shallow-water assemblages have been displaced into deep-water settings. Due to the presence of *Lingulodinium hemicystum* (first appearance data: 23.0 Ma.) and *Pentadinium laticinctum* (last appearance data: 11.6 Ma.) an age not older than Miocene and not younger than the Serravallian/Tortorian boundary for the Punta Basílica section is proposed.

Keywords Hyperpycnites · Palynofacies · Miocene · Cabo Viamonte Beds · Austral Basin · Argentina

Electronic supplementary material The online version of this article (<https://doi.org/10.1007/s10347-018-0535-2>) contains supplementary material, which is available to authorized users.

✉ Marcelo A. Martínez
martinez@criba.edu.ar

Mirta E. Quattrocchio
mquattro@criba.edu.ar

Daniela E. Olivera
daniela.olivera@uns.edu.ar

Juan J. Ponce
jponce@unrn.edu.ar

Noelia B. Carmona
ncarmona@unrn.edu.ar

Introduction

Palynofacies is defined as a distinctive assemblage of palynological organic matter thought to reflect a specific set of environmental conditions or to be associated with a characteristic range of hydrocarbon-generating potential (Tyson 1995). Organic matter is transported similarly to inorganic

¹ Instituto Geológico del Sur-Consejo Nacional de Investigaciones Científicas y Técnicas CONICET), Departamento de Geología (UNS), San Juan 670, B8000ICN Bahía Blanca, Buenos Aires, Argentina

² Departamento de Geología, Universidad Nacional del Sur, San Juan 670, B8000ICN Bahía Blanca, Buenos Aires, Argentina

³ Instituto de Investigación en Paleobiología y Geología-Consejo Nacional de Investigaciones Científicas y Técnicas (CONICET), Universidad Nacional de Río Negro, Isidro Lobo y Belgrano, 8332, General Roca, Río Negro, Argentina

grains, thus, the results of a particulate organic matter study should be correlated with the outcomes of a sedimentary study.

The present contribution combines the results of palynostratigraphic and quantitative palynofacies analysis in two localities included within the Cabo Viamonte Beds from the Austral foreland basin of Tierra del Fuego, Argentina (Fig. 1), showing that such an approach contributes to a more accurate and detailed stratigraphic and environmental interpretation. Information about the relations between palynomorph concentration and the biosphere association

such as vegetation types is given, and palynostratigraphical analysis, which uses the palynomorph content of a rock sample, allow determining its age.

In the study's localities the diagnostic criteria for the recognition of the hyperpycnal flows are recognized, that is, the transitional and recurrent (vertical and lateral) alternation between sedimentary structures without physical boundaries, associated with the co-occurrence of plant remains (*Nothofagus*) (Ponce and Carmona 2011a, b) (Fig. 2). Previous studies on palynology in probable hyperpycnal deposits from South America were done by

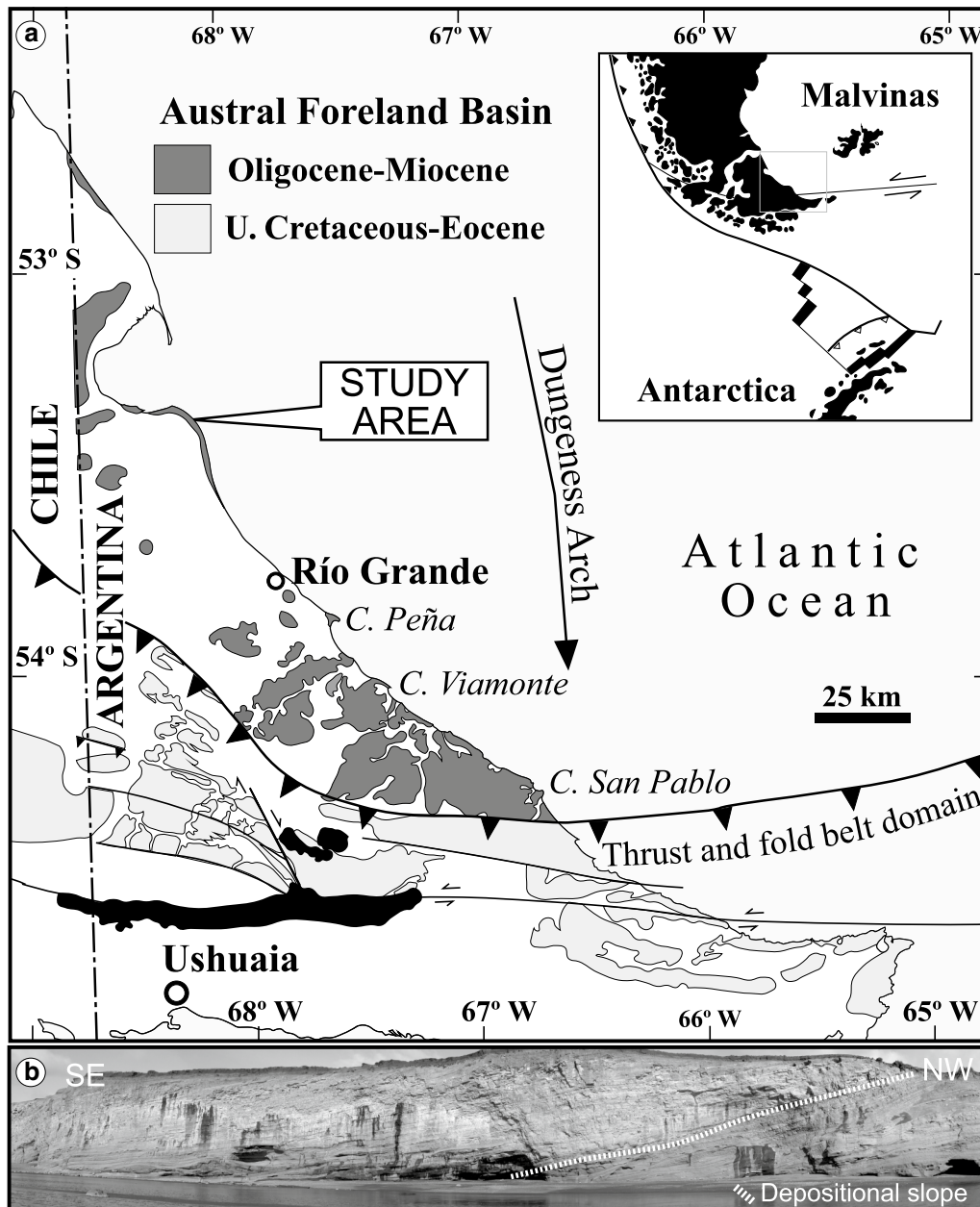


Fig. 1 **a** Simplified geologic map of Tierra del Fuego showing location of the study area in Punta Basílica. **b** Panoramic view of northwest-southeast-prograding sigmoidal clinoforms in Punta Basílica locality

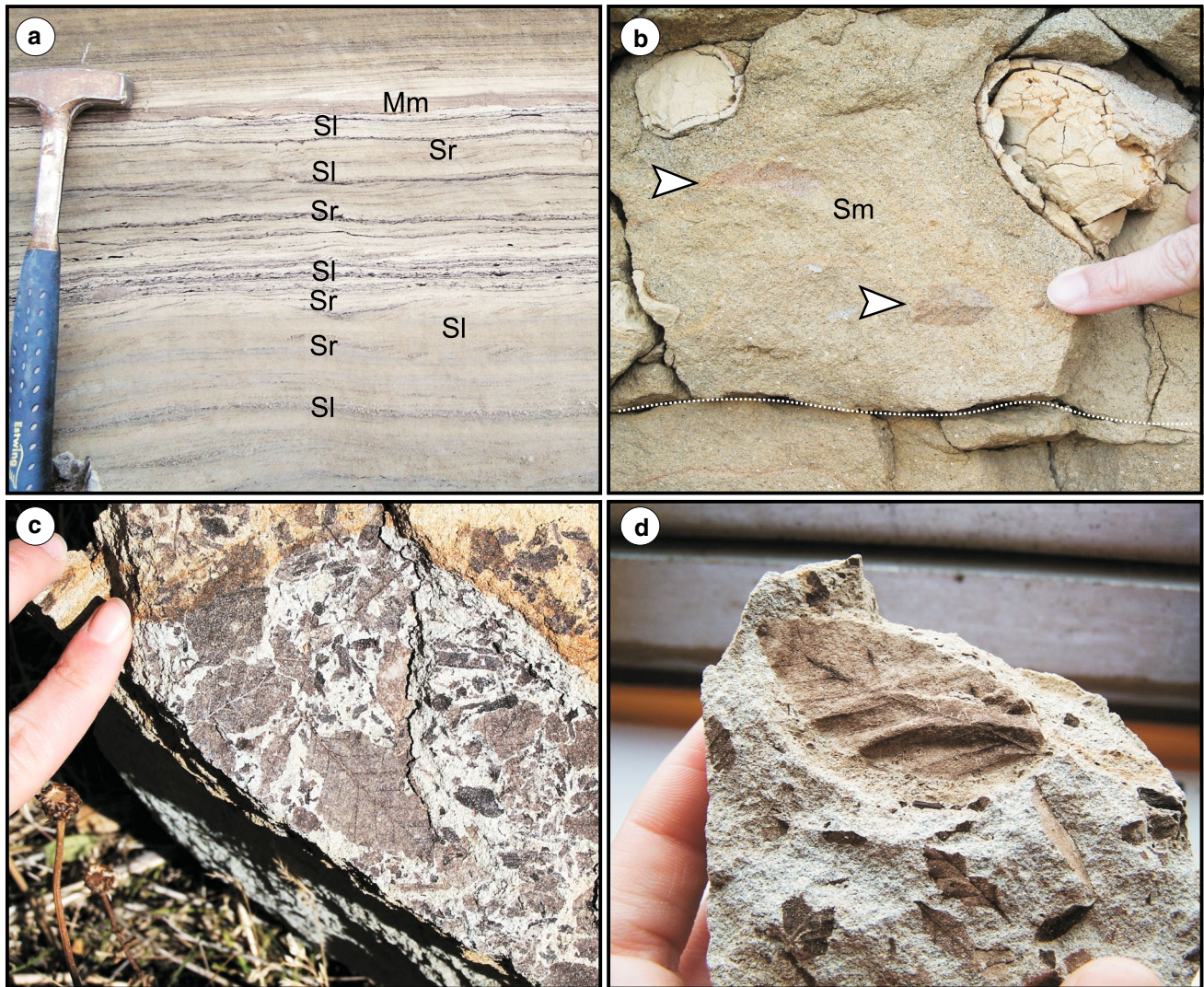


Fig. 2 **a** Heterolithic deposits showing recurrent transitions between sandstone with parallel lamination (SI), current ripples (Sr), and laminated or massive mudstone (M), with significant phytodetritus concentrations, reflecting fluctuations in flow velocity. **b** Massive sand-

stone facies (Sm) including chaotically distributed *Nothofagus* leaves (white arrows). **c**, **d** Detail of one level with leaves, note the deformation on the leaf surface in **d**, indicating that it was incorporated and transported fresh to the basin

Carrillo-Berumen et al. (2013) from the Paleogene Chorriillo Chico Formation (Magallanes Basin). Recently, Martínez et al. (2016) presented a taphonomic analysis of the palynological samples of prodelta hyperpycnites from the Los Molles and Lajas Formations (Middle Jurassic), Neuquén Basin. However, there are yet no detailed studies discussing the palynologic content in hyperpycnites. This contribution focuses on the analysis of the palynological organic matter behavior during the transport of the hyperpycnal flows, to characterize through the palynofacies analysis the related deposits in this clinoform system, and thereby to propose a palynofacies model applied to hyperpycnites.

Geologic setting

The geological evolution of the Austral Basin comprises three main tectonic phases: rift, sag, and foreland stages that evolved between the Jurassic and the Neogene times. The rift phase shows an extended bimodal volcanism, represented by the Upper Jurassic Lemaire (Tobífera) Formation, which rests unconformably on Paleozoic–Lower Jurassic rocks (Kranck 1932; Olivero and Martinioni 2001). The extensional regime produced the Rocas Verdes Marginal Basin, which was partially floored with ophiolites (Caminos et al. 1981; Ramos et al. 1986). This

basin, located between a Pacific volcanic arc to the south and America to the north, was filled with Early Cretaceous deep-marine turbidites of the Yahgan Formation and slope mudstones of the Beauvoir Formation (Olivero and Martinioni 2001). The sag phase is associated with a strong thermal subsidence and a maximum marine expansion during the latest Early Cretaceous (Biddle et al. 1986; Robbiano et al. 1996; Galeazzi 1998). During the early Late Cretaceous, a compressional tectonic regime caused the closure and tectonic inversion of the Rocas Verdes Marginal Basin (see Olivero and Martinioni 2001). In the Late Campanian (Olivero et al. 2003), this compressional regime led to the uplift of the Fuegian Andes and the following generation of the foreland Austral and Malvinas basins (Biddle et al. 1986) (Fig. 1a). A series of asymmetric clastic successions of Late Cretaceous–Danian; Late Paleocene–Early Eocene; late Mid Eocene–Late Eocene, and Oligocene–Early Miocene ages were accumulated as a result of the northern propagation of the compressional deformation, towards the foreland (Olivero and Malumián 2008). Since the Early Miocene, the marine sedimentation is represented by undeformed successions developed after cessation of the compressive deformation. These less-deformed marine deposits are mostly included within the Cabo Domingo Group (Malumián 1999). It reaches a minimum thickness of 1000 m of marine deposits, which are gradually changing from marine to marginal-marine towards the NW, and finally to continental deposits (uppermost Eocene–Mid Miocene; Malumián and Olivero 2006). To the northern part of the Austral Basin, the Upper Oligocene–Mid Miocene deep-marine strata of the Cabo Domingo Group correlate with shelf deposits of the marine “Patagonian” units (Monte León and Centinela Formations), and with the overlying continental deposits of the Santa Cruz Formation (Malumián and Náñez 1996; Malumián 1999; Malumián and Olivero 2006).

The youngest Austral Basin foredeep deposits shows two different types of basin infill, described as “Type a” and “Type b” clinoforms (Ponce et al. 2008). Type a clinoforms were active during the Paleocene–Middle Miocene, show major thicknesses close to the orogenic front and an abrupt thinning with onlap relationships towards the foreland, whereas Type b clinoforms (dominant since the Middle Miocene) show a marked sigmoidal geometry and lateral extensions of several kilometers.

The study area includes the deposits from Punta Basílica locality and one sample from Cabo Viamonte locality, located 90 km to the south from Punta Basílica (Fig. 1a), both included within the Cabo Viamonte Beds, Cabo Domingo Group (Late Eocene–Middle Miocene), in the Austral foreland basin of Tierra del Fuego, Argentina (Malumián and Olivero 2006). The Punta Basílica deposits correspond to the Type b clinoforms. In particular, the Type b

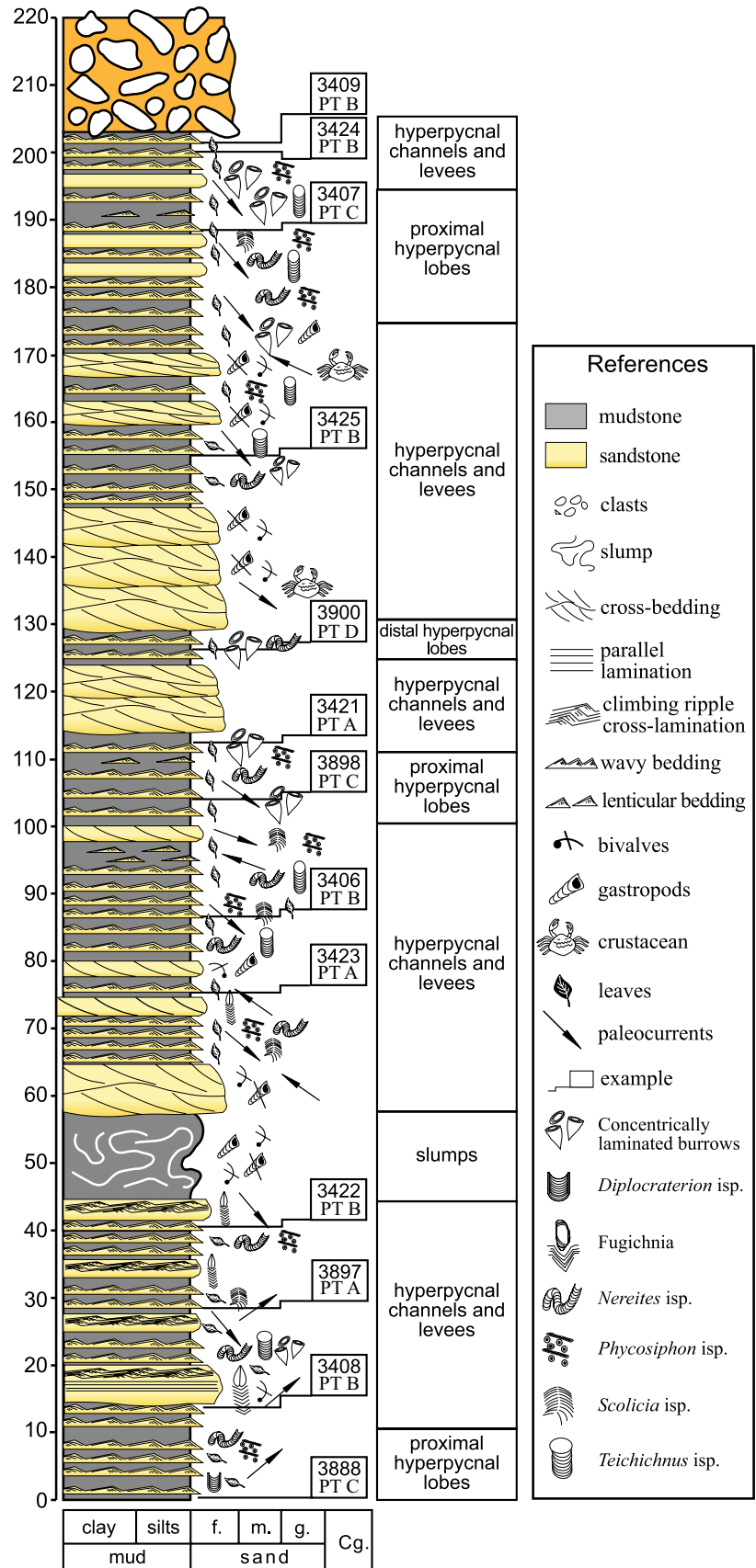
clinoforms are as much as 150 m thick, with a horizontal distance of 700 m from the edge of the topset to the beginning of the bottomset (Ponce and Carmona 2011a, b) (Fig. 1b). These deposits are mainly composed of conglomerates, gravelly sandstones, and massive sandstones, sandstones with climbing dunes, parallel lamination, climbing ripples, and laminated and massive mudstones, with abundant phyto-detritus, well-preserved *Nothofagus* leaves, and bioclasts, mainly concentrated in sandstone and mudstone facies. Internally, these deposits show reverse to normally gradation, and transitions and recurrence of tractive sedimentary structures with evidence of bedload transport (Fig. 2). Mulder et al. (2003) and Zavala et al. (2006) described similar sedimentary facies arrangements for deposits of different ages, attributing them to hyperpycnites. The presence of well-preserved *Nothofagus* leaves in the thick massive sandstone beds suggests direct terrestrial input into the basin (Plink-Björklund and Steel 2004). Paleogeographic reconstructions suggest that the Cabo Viamonte Beds comprise two dominant architectural elements, channel-levee and lobe complexes, formed mainly by density hyperpycnal currents in outer shelf to deep-marine environments (Ponce and Carmona 2011a).

Materials and methods

Fieldwork included the measurement of a 200 m thick section consisting of sandy and muddy heterolithic deposits with subordinated sandstone beds accumulated at the toe of clinoform systems (Figs. 1b, 3), and a detailed palynological sampling of the heterolithic material. The present study focused on 14 samples, 13 from the Punta Basílica locality (samples 3406–3409, 3421–3425, 3888, 3897–3898, 3900) and one from the Cabo Viamonte locality (sample 3899) (Figs. 1a, 3). Physical and chemical extraction of the samples was performed using standard palynological processing techniques (Volkheimer and Melendi 1976), which involve treatment with hydrochloric and hydrofluoric acids. No oxidation by nitric acid was performed because it affects the fluorescence of the hydrogen-rich particles. It is worthy to mention that the palynofacies analysis work done herein is based only on palynofacies (i.e., unoxidized) slides. The palynological slides are housed at the Instituto Geológico del Sur-Universidad Nacional del Sur, Bahía Blanca, Buenos Aires province, Argentina, under the repository code UNSP (Universidad Nacional del Sur, Palynology). The specimen locations are referred to England Finder coordinates.

The statistical count (at least 500 particles per sample) is necessary to determine the general character of the particulate sedimentary organic matter: SOM (Batten 1996). These counts constitute the base to that accurate palaeoenvironmental interpretations can be performed. The relative

Fig. 3 Measured section in Punta Basilica locality, showing the sedimentological and ichnologic characteristics, the locations of the palynological sampling and the palynofacies types (PT)



frequencies (%) diagram was calculated using TGview 2.0.2 (Grimm 2004). Each sedimentary facies is characterized by its palynological organic matter content, recognized in transmitted white light and incident blue light fluorescence. The classifications of Tyson (1995), Batten (1983), and Oboh-Ikuenobe and de Villiers (2003) of the palynological organic matter are used herein. Seventeen organic matter types were distinguished for palynofacies analysis categorized in five major groups, amorphous organic matter (AOM), palynomorphs (Fig. 4a–r), fungal remains (Fig. 4s–w), zooclasts and phytoclasts (Fig. 4x–z). In addition, the degree of alteration of the palynological assemblages was also evaluated by examination of the state of preservation of palynomorphs in the sediment samples ('deterioration classes' of Delcourt and Delcourt 1980).

The palynofacies analysis was employed using the multivariate statistical program PAST (Palaeontological Statistics) by Hammer and Harper (2009). Cluster analysis (Q-mode) was utilized based on the composition and abundance (number of elements) in order to establish groupings of samples and to recognize the different associations of the palynological organic matter (palynofacies type). It was performed with the Euclidean distance and the unweighted pair group method (UPGM). Palynofacies types (PT) are defined on the quantitative total organic matter data, and may reveal important information for paleoenvironmental interpretation (Brugman et al. 1994 and references therein) (Table 1). The list of identified species and its natural affinities of the dispersed palynomorphs are summarized in Table 2.

Results

Palynofacies analysis

The most conspicuous feature of all identified palynofacies types is the dominance of the phytoclast group, varying from 47.5 to 98% of the total organic matter (ESM A1). However, taking into account the relative variations of the 17 organic matter types, the samples are assigned to four PT by cluster analysis: A, B, C, and D (Figs. 5, 6; Table 1).

Palynofacies type A. Woody/brown to black phytoclasts + AOM. Samples 3899, 3897, 3423, 3421

This presents the highest percentages of phytoclasts in all palynofacies (86.4–99.4%; Fig. 5). It is characterized by the predominance of tissues, tracheids, woods (55–74%), and dark brown to black phytoclasts (20–30%), with spongy amorphous organic matter (up to 6%) (Fig. 5). Sample 3421 presents framboidal pyrite and sample 3423 contains palynomorphs with mechanical damage. The palynomorphs are scarce and mostly of terrestrial origin (fungi, ferns,

Nothofagaceae and Botryococcaceae). The recorded spores correspond mainly to fungi and the scant recognized fern spores belong to *Biretisporites* sp., *Laevigatospories ovatus*. Among the pollen grains, Haloragaceae (*Myriophyllum* sp.) and Nothofagaceae are observed. The organic-walled marine microplankton (OWMM) is represented by prasinophycean algae (*Cymatiosphaera* sp.) and indeterminate dinoflagellate cysts. The 3899 and 3897 are barren in palynomorphs.

This PT has been recorded in muddy heterolytic deposits, which have also yielded leaves and seeds belonging to the channel and levee zone (Fig. 3).

Palynofacies type B. Pollen + spores/yellow to brown phytoclast. Samples 3408, 3422, 3406, 3425, 3424, and 3409

This type is characterized by the highest percentages of fungal remains (up to 40%) identified in all of the studied samples. Fungal spores make up to 18% of the total organic matter. Woods, tracheids, and tissues (WTT) show high percentages, reaching up to 53% and the yellow to pale brown phytoclasts represent up to 29% (Fig. 5). Among the palynomorph group, the terrestrial forms are dominant, mainly represented by pollen grains of Podocarpaceae (*Podocarpidites marwickii*), Araucariaceae (*Araucariacites australis*), Nothofagaceae (*Nothofagidites dorotensis*, *N. rocaensis*), Poaceae, and others (Fig. 4). Samples 3424 and 3425 show the greatest pollen diversity. The continental algae are represented by structureless *Botryococcus* colonies. The OWMM is represented by dinoflagellate cysts (*Batiacasphaera baculata*, *Pentadinium* cf. *laticinctum*, and *Lingulodinium* sp.) (Fig. 4).

The PT B has been recorded from muddy and sandy heterolithic deposits belonging to the channel and levee zone (Fig. 3).

Palynofacies type C. Brown to black phytoclasts/AOM. Samples 3407, 3888, and 3898

This PT shows the highest percentage of dark brown to black fragments (42–57%) in all studied samples, with the maximum of equidimensional opaque particles (7.1%) in the 3888 sample (Fig. 5). High values of WTT (14–29%) are also registered in this unit. Sample 3898 is the only level with granular AOM (22%). In general, palynomorphs are scarce being represented by members of the families Polypodiaceae (*Notholaena mollis*), Asteraceae, Proteaceae, Nothofagaceae, Poaceae, and others.

This PT has been recovered from muddy and sandy heterolithic deposits identified in proximal hyperpycnal lobe facies (Fig. 3).

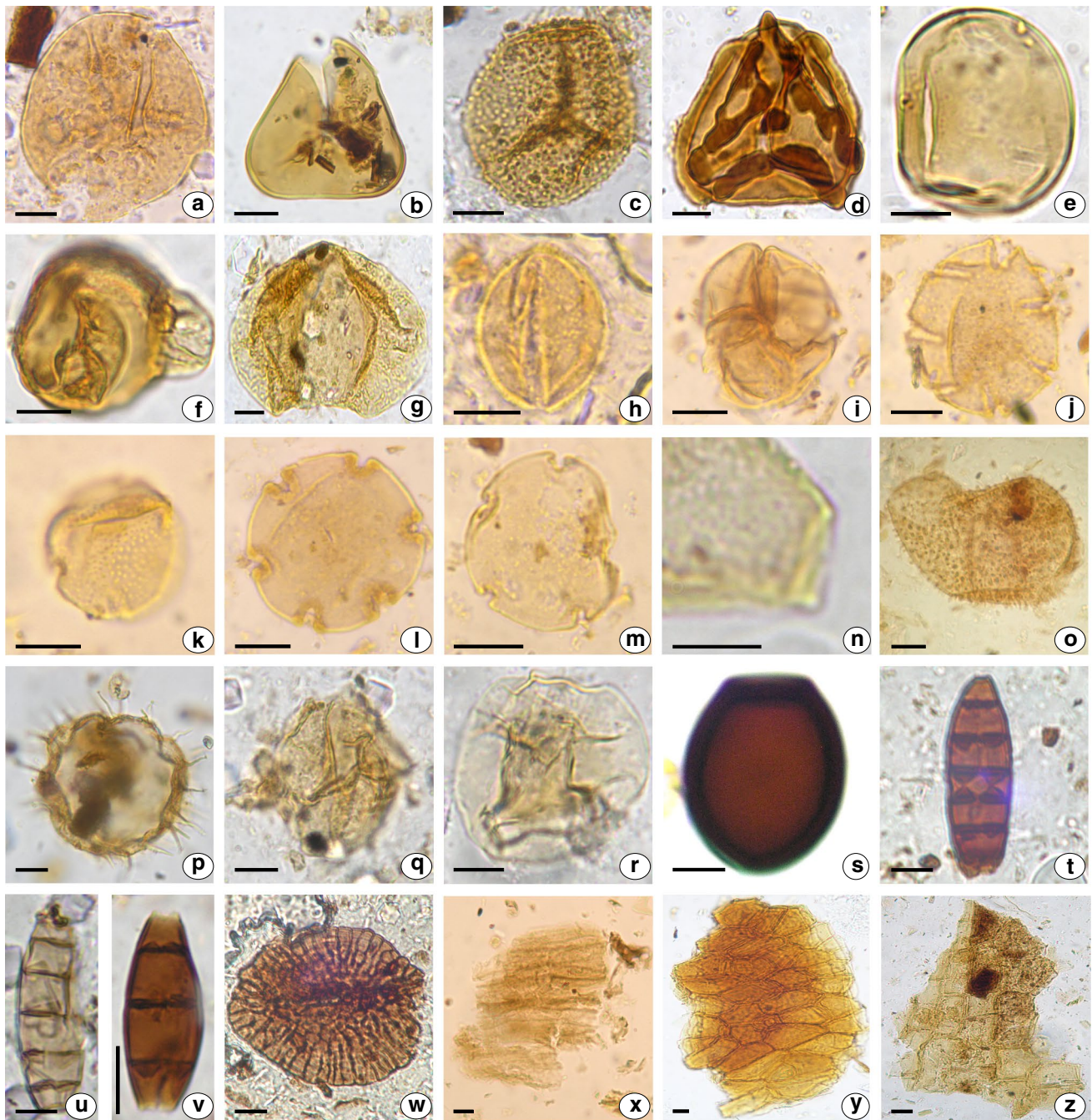


Fig. 4 Scale bar, 10 μm . **a** *Notholaena mollis* (Kunze) Presl, 3407: O26/0; **b** *Deltoidospora australis* (Couper) Pocock, 3425: K33/0; **c** *Baculatisporites turbioensis* Archangelsky, 3408: P27/0; **d** *Klukisporites* sp., 3422: M24/0; **e** *Laevigatosporites ovatus* Wilson and Webster, 3425: H68/1; **f** *Phyllocladidites mawsonii* Cookson, 3425: B36/1; **g** *Podocarpidites marwickii* Couper, 3409: Z73/2; **h** Asteraceae, 3407: B47/3; **i** *Myrica/Empetrum*: 3423: K35/4; **j** *Nothofagidites flemingii* (Couper) Potonié, 3422: V39/4; **k** *Nothofagidites nanus* Romero, 3425b: P29/2; **l** *Nothofagidites rocaensis* Romero, 3423:

B37/1; **m** *Nothofagidites saraensis* Menéndez and Caccavari, 3422: T37/1; **n** *Proteacidites symphonemoides* Cookson, 3425b: K34/0; **o** *Batiacasphaera baculata* Drugg, 3408b: G24/4; **p** *Lingulodinium hemicystum* McMinn 3409b: C57/3; **q** *Pentadinium laticinctum* (Gerlach) Benedek et al., 3409: V31/1; **r** *Thalassiphora pelagica*; 3900: J33/2; **s** *Lacrimasporonites* sp., 3408a: A29/0; **t** *Fractisporonites* sp. A, 3408b: S75/0; **u** *Fractisporonites* sp. B, 3408b: S75/0; **v** *Diporites* sp., 3406b: A39/1; **w** Microtiriaceae, 3407b: O32/0; **x** woody debris, 3425b: C39/4; **y**, **z** cuticle, 25. 3425b: P46/0; 26. 3408b: B42/3

Table 1 Palynofacies types identified after the cluster analysis

Palynofacies types	Description
A	
Woody + brown to black phytoclasts/AOM	Predominance of tissues, woody debris and brown to black phytoclasts with spongy amorphous
B	
Pollen + spores/yellow to brown phytoclasts	Predominance of spores followed by pollen grains, continental algae, hyphae and tissues. Dominance of yellow to brown phytoclasts. Spongy amorphous
C	
Brown to black phytoclasts/AOM	Dominance of brown to black phytoclasts with equidimensional opaque particles. Moderate content of spongy to fibrous amorphous. In 3898 granular AOM
D	
Pollen + spores/opaque phytoclasts + brown to black phytoclasts	Predominance of pollen grains followed by spores. Dominance of equidimensional opaque particles and blade shape and brown to black phytoclasts

Palynofacies type D. Pollen + spores/opaque phytoclasts + brown to black phytoclasts. Sample 3900

The highest percentages of palynomorphs (18.4%) and the maximum registered value of the opaque equidimensional particles (50.5%) characterize this type. Even though the lath-shaped particles have not reached high absolute percentages, they show the maximum value observed in all studied samples (Fig. 5; ESM A1). Among the palynomorphs there is a predominance of pollen grains (14%) followed by bryophyte and pteridophyte spores (3%). The pollen grains are represented by abundant Nothofagaceae (50% of the total pollen grain sums), with subordinate Podocarpaceae (12% of the total pollen grains sums). *Batiacasphaera* spp., *Operculodinium centrocarpum*, *Spiniferites* spp., and *Thalasisphora* sp. are registered as the more common taxa among the dinocysts, reaching up 2%.

This SOM was preserved in massive mudstones recognized in distal hyperpycnal lobe facies (Fig. 3).

Biosphere association and palynostratigraphy

The biosphere association from which the palynological fossils were derived corresponds to 37 taxa of spores, pollen grains, dinoflagellate cysts, algae, and acritarchs (Table 2). The palynological information indicates that in the continent, the forest was dominated by Podocarpaceae, Nothofagaceae, and Araucariaceae, with fern communities (Fig. 4). Open habitat families are also present (Poaceae, Asteraceae, and Ephedraceae). The absence of megatherm elements like Arecaceae, Symplocaceae, and the presence of arid-loving taxa such as Ephedraceae, Asteraceae, and Proteaceae, suggest an age not older than Late Aquitanian (Barreda and Palazzesi 2014) for the present assemblage. Botanical information indicates that during the earliest Miocene many modern taxa appeared and diversified, contributing to a more complex vegetation structure with patches of open and dry-tolerant taxa. These communities characteristic of

Early Miocene deposits (Barreda and Palazzesi 2014) are present in the analyzed section.

Due to the presence of *Lingulodinium hemicystum* (first appearance data: 23.0 Ma.) and *Pentadinium laticinctum* (last appearance data: 11.6 Ma.) an age not older than Early Miocene and not younger than the Serravallian/Tortonian boundary is proposed for the Punta Basílica section.

Discussion

Classic turbidites result from turbidity currents originated within the marine basin, so their deposits are in general termed “intra-basinal turbidites”. Instead, the deposits of turbidity currents initiated in the continental realm during river floods (hyperpycnal flows) are termed “extra-basinal turbidites” (see Zavala and Arcuri 2016). In this section, we discuss some basic concepts about the hyperpycnal flows as an effective mechanism for the basinward transport of the freshwater and plant debris for long distances, as long as the river discharge continued during floods. We will discuss the result organic association (palynofacies type) recovered from these hyperpycnites (hyperpycnal flow deposits). At present, studies focused on the palynological content of hyperpycnites are scarce (e.g., Biscara et al. 2011; Carrillo-Berumen et al. 2013; Martínez et al. 2016; Mignard et al. 2017; Slater et al. 2017).

In intra-basinal turbidite systems, the basal coarse-grained facies are dominated by terrestrially organic matter, whereas the upper fine-grained divisions are characterized by AOM and marine palynomorphs (Tyson 1995 and references therein). On the contrary, in hyperpycnites, plant remains occur in most of their facies (e.g., in massive sandstones, sandstones with climbing dunes, parallel lamination, climbing ripples, and laminated and massive mudstones) (Ponce and Carmona 2011a, b; Zavala et al. 2012).

The hyperpycnal deposits from Cabo Viamonte Beds are characterized by the presence of large tree-trunks with

Table 2 Natural affinities of spores, pollen grains, fungi and organic-walled microplankton

Taxon	Natural affinity
Bryophyte and fern spores	
<i>Baculatisporites turbioensis</i> Archangelsky 1972	Osmundaceae
<i>Biretisporites</i> sp.	?Osmundaceae
<i>Notholaena mollis</i> (Kunze) Presl 1836	Pteridaceae
<i>Deltoidospora australis</i> (Couper) Pocock 1970	Polypodiaceae/Cyatheaceae
Hymenophylleaceae	Hymenophyllaceae
<i>Klukisporites</i> sp.	Schizaceae
<i>Laevigatosporites ovatus</i> Wilson and Webster 1946	Blechnaceae
<i>Matonisporites ornamentalis</i> (Cookson) Partridge in Stover and Partridge 1973	Dicksoniaceae
Gymnosperm pollen grains	
<i>Araucariacites australis</i> Cookson 1947	Polypodiaceae
<i>Araucariacites australis</i> Cookson 1947	Araucariaceae
<i>Ephedripites</i> sp.	Ephedraceae
<i>Phyllocladidites mawsonii</i> Cookson 1947	Podocarpaceae
<i>Podocarpidites ellipticus</i> (Cookson) Couper 1053	Podocarpaceae
<i>Podocarpidites rugulosus</i> Romero 1977	Podocarpaceae
<i>Podocarpidites marwickii</i> Couper 1953	Podocarpaceae
<i>Taxodiaceapollenites hiatus</i> (Potonie) Kremp	Taxodiaceae
Angiosperm pollen grains	
Asteraceae	Asteraceae
<i>Graminidites</i> sp.	Poaceae
<i>Myrica/Empetrum</i>	Myricaceae/Empetraceae
<i>Haloragacidites</i> sp.	Haloragaceae
<i>Nothofagidites anisoechinatus</i> Menéndez and Caccavari 1975	Nothofagaceae
<i>Nothofagidites dorotensis</i> Romero 1973	Nothofagaceae
<i>Nothofagidites flemingii</i> (Couper) Potonié 1960	Nothofagaceae
<i>Nothofagidites rocaensis</i> Romero 1973	Nothofagaceae
<i>Nothofagidites saraensis</i> Menéndez and Caccavari 1975	Nothofagaceae
<i>Proteacidites subscabratus</i> (Couper) Harris 1965	Proteaceae
<i>Proteacidites symphyonemoides</i> Cookson 1950	Proteaceae
<i>Psilatricolporites</i> sp.	
<i>Rhoipites minusculus</i> Archangelsky 1973	Loganiaceae
Organic walled marine microplankton	
<i>Batiacasphaera baculata</i> Drugg 1970	Dinoflagellata
<i>Batiacasphaera</i> spp.	Dinoflagellata
<i>Kallosphaeridium</i> sp.	Dinoflagellata
<i>Lingulodinium hemicystum</i> McMinn 1991	Dinoflagellata
<i>Pentadinium laticinctum</i> (Gerlach) Benedek et al. 1982	Dinoflagellata
<i>Spiniferites</i> spp.	Dinoflagellata
<i>Thalassiphora pelagica</i> (Eisenack) Eisenack and Gocht 1960	Dinoflagellata
Algae	
<i>Botryococcus</i> sp.	Botryococcaceae
<i>Ovoidites</i> sp.	Zygnemataceae
Acritarchs	
<i>Leiosphaeridia</i> spp.	
<i>Cymatiosphaera</i> sp.	
Fungi	
<i>Diporites</i> sp.	
<i>Fractisporonites</i> sp. A	
<i>Fractisporonites</i> sp. B	
<i>Lacrimasporonites</i> sp.	
Microtiriaceae	

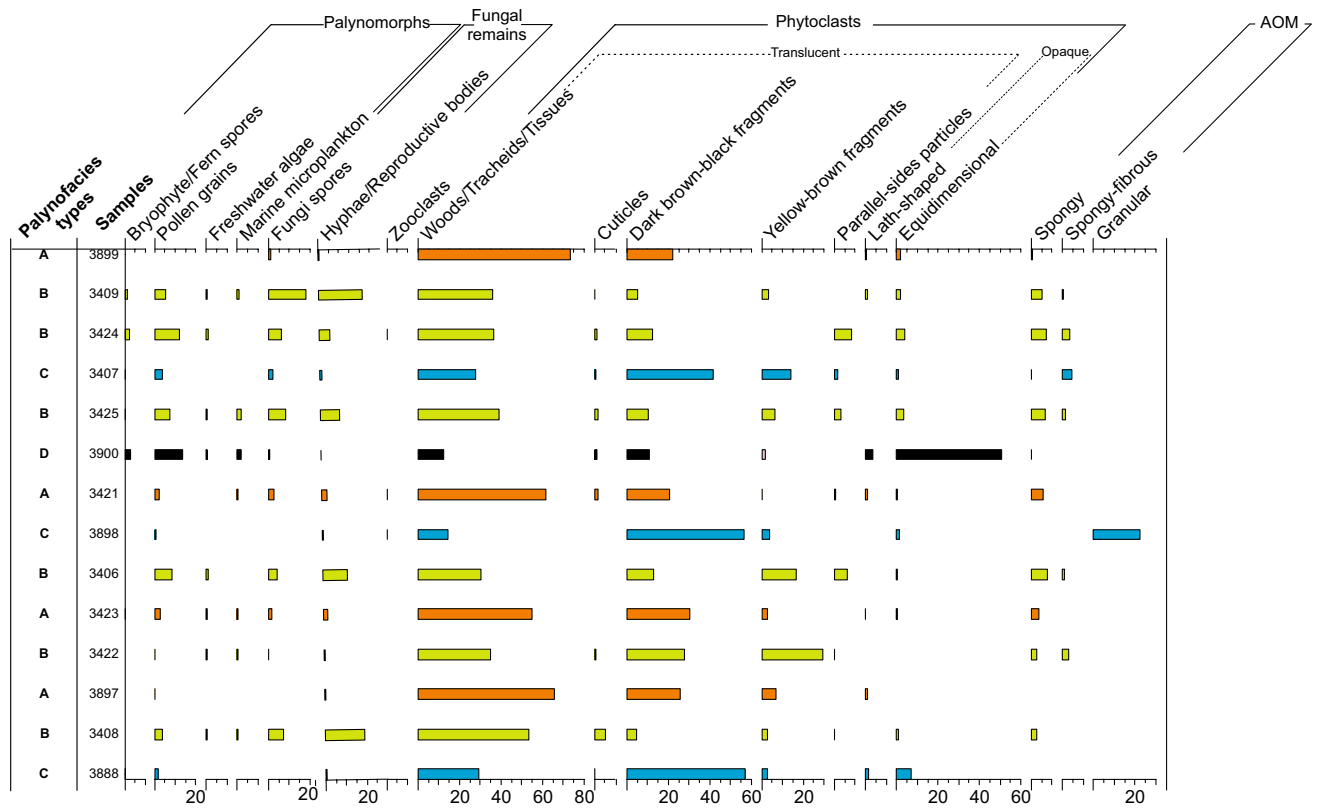


Fig. 5 Quantitative distribution of particulate sedimentary organic matter (SOM) expressed in percentages in samples of the Cabo Viamonte Beds, Cabo Domingo Group

abundant leaves (*Nothofagus*) and particulate organic matter coming from the continent. In the recognized palynofacies types (Table 1), the main marine components are dinoflagellate cysts. The AOM seems in general to come from the alteration of tissues (spongy to fibrous, not fluorescent with UV filter), although in the sample 3898, the granular AOM seems to come from degraded algal/bacterial constituents (after Batten 1983; Pacton et al. 2011).

In a turbidity current (s.l.), organic particles act as sedimentary particles, with sorting and settling velocity largely controlled by particle size, density, shape, and texture (McArthur et al. 2016). Therefore, the lighter material in these flows may have the greatest potential for long-distance transportation (Tyson and Follows 2000).

Proximal–distal trends clearly emerge when taking into account the organic matter content in the four palynofacies types recognized in this contribution (Fig. 7).

The highest percentages of fungal remains (spores plus hyphae) are observed in the PT B. This might be related to a relatively more proximal position from the source area of this palynofacies. Fungal spores are less wind-transported because they are generally produced in the thick mats of the decaying plant material (Ratan and Chandra 1983).

The outer wall of the fungal sclerotium is commonly thickened and heavily melanized (and thus darkly pigmented), increasing their density, which promotes their accumulation in relatively proximal facies (Table 3). In the modern Orinoco Delta, fungal spores are most abundant in delta top facies (in Tyson 1995, p. 280). The important presence of fresh phytoclasts (yellow to pale brown fragments) suggests that these particles would have remained for a short period of time in contact with oxidizing waters. All the characteristics of PT B correspond to the most proximal position among of the four studied palynofacies types (Fig. 7).

In PT A, an increase in the frequencies of structured phytoclasts (WTT) is observed, black to dark-brown fragments and lath-shaped opaque phytoclasts, while cuticles and yellow to pale-brown fragments decrease, compared to PT B (Fig. 5; ESM A1). This gives evidence for a more distal position of PT A (Fig. 7). These palynofacies types have been recorded from channel and levee facies of a hyperpycnite. Some authors (e.g., Zavala and Arcuri 2016) propose that in the channel zone these currents behave as a fluid flow allowing the normal sorting of the clastic and organic particles. This could explain the proximal–distal

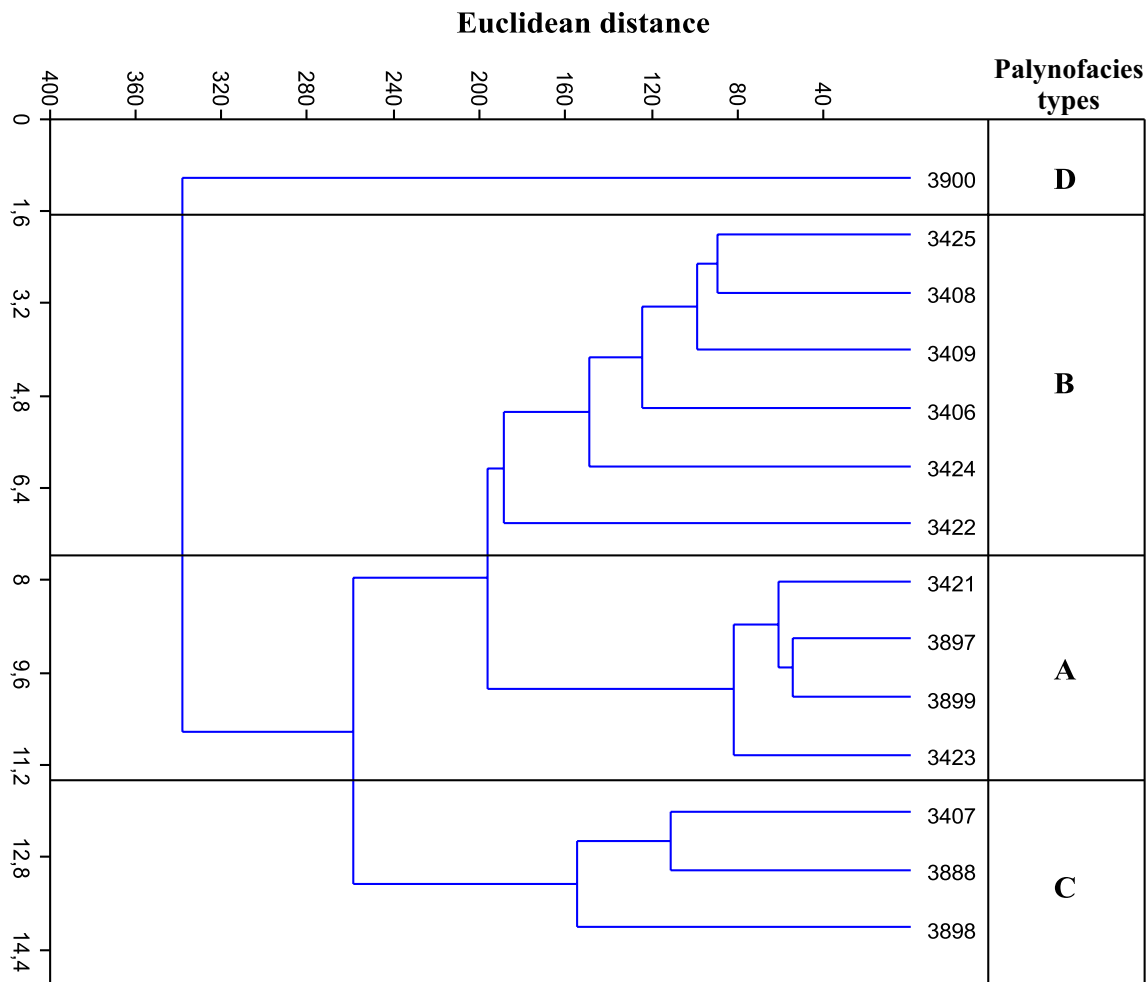


Fig. 6 Cluster analysis, using Euclidean distance and the unweighted pair group method (UPGM), showing the grouping of the identified palynofacies types

trend observed in both palynofacies types sensu Tyson (1995, Table 25.3).

When the turbulent flow decreases its density by deposition of the material transported by turbulence, a rising turbulent plume (lofting plume) charged with the remaining very fine-grained sand-silt size particles together with lighter elements (micas and plant debris) is produced (Zavala and Arcuri 2016). When these materials are mixed with the marine waters, the lofting plume progressively dissipates with the consequent deposition by the free fall-out of the suspended material, according to the Stokes' law (Fig. 7; Table 3). The PT D has been recovered in the lofting facies and shows the highest percentages of palynomorphs of all studied samples. Among this group, the *Nothofagaceae* pollen grains reach up to 50% of the total spectrum. This pollen type, which is relatively small, would have been carried further offshore to the sea than larger sporomorphs from similar source areas. In this case, *Nothofagus* may act as a clastic component, sensitive to

increments of the sedimentary input. Moreover, the maximum value of lath-shaped opaque organic particles is observed also in this PT suggesting an offshore environment (Parry et al. 1981; Gorin and Steffen 1991; Martínez et al. 2008 among others) (Fig. 5). The highest frequencies of equidimensional opaque particles could be explained by the free fallout of the suspended particles, this behavior would only be expected in distal mudstone facies related to the lofting plume (Fig. 7). The organic-walled marine microplankton content shows the co-occurrence of inshore species (e.g., *Batiacasphaera* spp., *Lingulodinium* spp.) with relatively more oceanic species (e.g., *Operculodinium centrocarpum*, *Spiniferites* spp.). The mixture of the neritic and oceanic taxa in a single association gives evidence that shallow-water assemblages have been displaced into a deep-water setting.

Carrillo-Berumen et al. (2013) proposed for the Chorrillo Chico Formation (Paleogene), Punta Prat locality (Magallanes/Austral Basin), a hyperpycnal origin by these deposits.

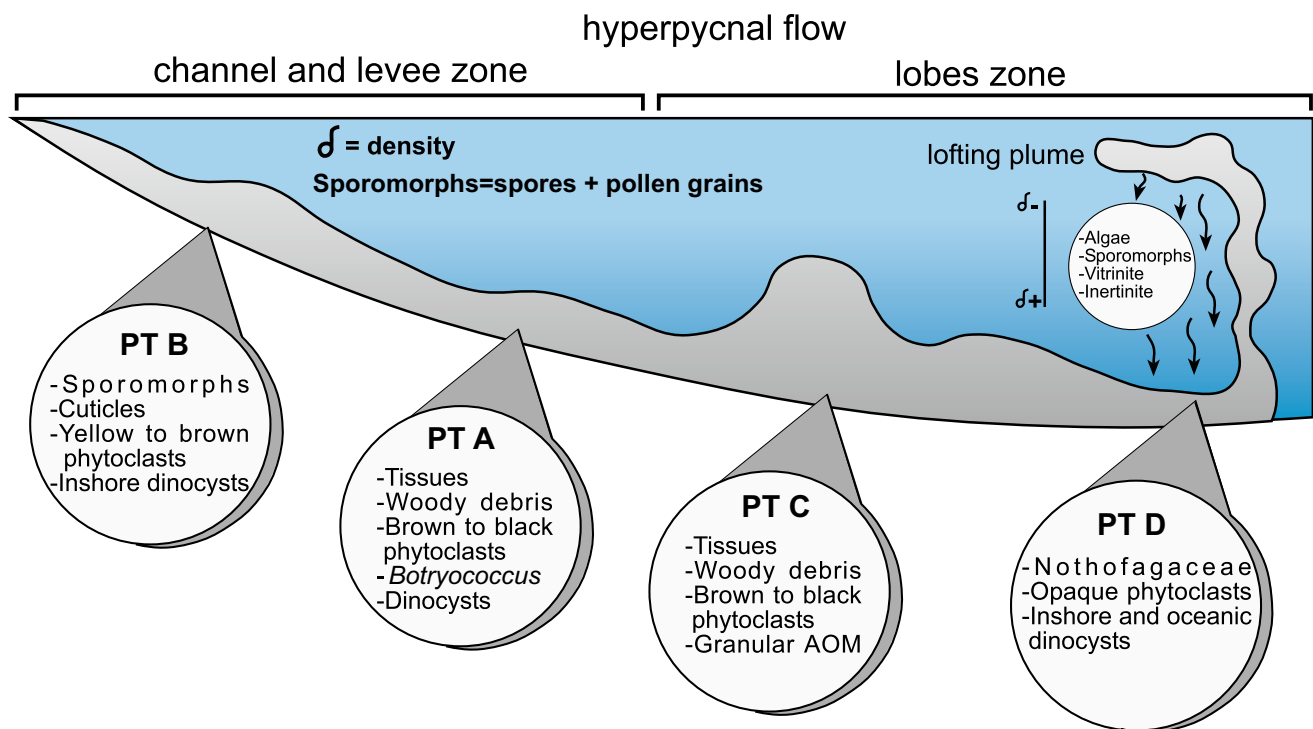


Fig. 7 Model of formation of hyperpycnal flow with palynofacies types

Table 3 Density of ancient sedimentary organic matter (after Tyson 1995)

Category	Source	Constituent	Maceral group	Density
Palynomorphs	Freshwater algae	<i>Botryococcus</i>	Liptinite or exinite	0.96
	Dinoflagellates	Dinocyst		1.1–1.3 ^a
	Sporomorphs	Spores and pollen		1.1–1.2
Fungal remains	Fungi	Spores and hyphae	Sclerotinite	1.6–2.0
Phytoclasts	Macrophyte plant debris	Cuticle	Liptinite	1.15–1.25
		Wood	Vitrinite	1.25–1.4
		Yellow to brown fragments		
		Dark brown to black fragments		1.25–1.7
		Opaque phytoclasts	Inertinite	1.3–1.45
Amorphous	Phytoplankton or bacterially derived	AOM	Liptinite or exinite	1.15–1.25
	Higher plant decomposition products		Vitrinite or huminite	1.25–1.4

^aModern organic matter

These authors report a high abundance of sporomorphs, which indicates the proximity of a fluvial source, together with the great diversity and abundance of dinoflagellate cysts (e.g., the presence of the genus *Impagidinium*) that indicates deposition in an external shelf. Similar behavior had been registered in the PT D.

In PT C, recorded from proximal hyperpycnal lobe facies, it is important to highlight the coexistence of the highest percentages of dark-brown to black fragments with the

maximum value of granular AOM of all studied samples (Fig. 5). The mixture of autochthonous marine organic matter (granular AOM) with terrestrial material may be related to the deposition of amorphous matter on the seabed during the quiescence period between consecutive hyperpycnal events, which mixed the autochthonous components with terrestrial allochthonous material carried within the hyperpycnal flow (Stetten et al. 2015).

Conclusions

Considering the stratigraphic range of the identified sporomorphs and dinoflagellates cysts, a Late Aquitanian to the Serravallian/Tortonian boundary interval is suggested as the time of deposition of the sediments in the Punta Basílica Section.

Four palynofacies types (A–D) were recognized after the cluster analysis of sandy and muddy heterolithic deposits. They reflect different positions within a hyperpycnal depositional system (from channel-levee to lobe complexes deposits), which correspond to different reworking and sorting of the SOM (size selection and density) during the transport and deposition.

The studied palynofacies show predominance of spores and pollen grains, phytoclasts, and spongy and fibrous amorphous organic matter (plant- and/or freshwater algae-derived), which reflect a high continental input to the basin, related to the discharge of hyperpycnal flows.

The co-occurrence of inshore (*Batiacasphaera* spp., *Lingulodinium* sp.) with relatively more oceanic (*Operculodinium centrocarpum*, *Spiniferites* spp.) dinocysts is an evidence that shallow-water associations have been resuspended, incorporated into the hyperpycnal flow and displaced to deep-water marine environments.

Acknowledgements We thank S. Candel, F. Ponce and M. Espié for their assistance during field work. The authors kindly acknowledge the reviews of Hartmut Jäger and George R. Dix and the comments of Editor-in-Chief Axel Munnecke, which improved the final version of the manuscript. Financial support was provided by Consejo Nacional de Investigaciones Científicas y Técnicas following Research Project: (PIP 417); Agencia Nacional de Promoción Científica y Tecnológica (PICT 2011-1373); Agencia Nacional de Promoción Científica y Tecnológica-Universidad Nacional de Río Negro (PICTO-UNRN 2010-0199) and Secretaría General de Ciencia y Tecnología de la Universidad Nacional del Sur (PGI-24/H142).

References

- Barreda VD, Palazzesi L (2014) Response of plant diversity to Miocene forcing events: the case of Patagonia. In: Stevens WD, Montiel OM, Raven PH (eds) Paleobotany and biogeography: a festschrift for Alan Graham in his 80th year. Monographs in systematic botany, vol 128. Ann Missouri Bot Gard Press, St. Louis, pp 1–25
- Batten DJ (1983) Identification of amorphous sedimentary organic matter by transmitted light microscopy. In: Brooks J (ed) Petroleum geochemistry and exploration of Europe. Geol. Soc. Spec. Pub., vol 12. The Geological Society/Blackwell, Oxford, pp 275–288
- Batten DJ (1996) Chapter 26. Palynofacies. Introduction. In: Jansonius J, McGregor DC (eds) Palynology: principles and applications, vol 3. AASP, Dallas, pp 1011–1064
- Biddle KT, Uliana MA, Mitchum RM Jr, Fitzgerald M, Wright RC (1986) The stratigraphic and structural evolution of the central and eastern Magallanes Basin, southern South America. In: Allen PA, Homewood P (eds) Foreland basins, vol 8. Ass Sediment Spec Publ, Belgium, pp 41–61
- Biscara L, Mulder T, Martinez P, Baudin F, Etcheber H, Jouanneau JM, Garlan T (2011) Transport of terrestrial organic matter in the Ogooué deep sea turbidite system (Gabon). Mar Pet Geol 28(5):1061–1072
- Brugman WA, van Bergen PF, Kerp JHF (1994) A quantitative approach to Triassic palynology: the Lettenkeuper of the Germanic Basin as an example. In: Traverse A (ed) Sedimentation of organic particles, vol 19. Cambridge Univ Press, New York, pp 409–429
- Caminos R, Haller M, Lapido J, Lizuain O, Page A, Ramos V (1981) Reconocimiento geológico de los Andes Fueguinos; Territorio Nacional de Tierra del Fuego. In: 8th Congreso Geológico Argentino, San Luis, Proceedings, vol 3, pp 759–786
- Carrillo-Berumen R, Quattrocchio ME, Helenes J (2013) Palinomorfos continentales del Paleógeno de las formaciones Chorrillo Chico y Agua Fresca, Punta Prat, Región de Magallanes, Chile. Andean Geol 40(3):539–560
- Delcourt PA, Delcourt HR (1980) Pollen preservation and Quaternary environmental history in the southeastern United States. Palynology 4:215–231
- Galeazzi JS (1998) Structural and stratigraphic evolution of the Western Malvinas basin, Argentina. Am Assoc Pet Geol B 82:596–636
- Gorin GE, Steffen D (1991) Organic facies as a tool for recording eustatic variations in marine fine-grained carbonates-example of the Berriasian stratotype at Berrias (Ardèche, SE France). Palaeogeogr Palaeoclimatol Palaeoecol 85:303–320
- Grimm E (2004) TGView 2.0.2. Springfield (IL): Illinois State Museum. Research and Collection Center
- Hammer O, Harper D (2009) PAST: paleontological statistics software package for education and data analysis. Version 1.94b. Paleontol Electrón 4(1):9
- Kranck EH (1932) Geological investigations in the Cordillera of Tierra del Fuego. Acta Geogr 4:1–231
- Malumián N (1999) La sedimentación y el volcanismo terciarios en la Patagonia extraandina. La sedimentación en la Patagonia extraandina. In: Caminos R (ed) Geología Argentina, Anales 29. Servicio Geológico Minero Argentino. Instituto de Geología y Recursos Minerales, San Martín, pp 557–612
- Malumián N, Nández C (1996) Microfósiles y nanofósiles calcareos de la plataforma continental. In: Ramos VA, Tunic MA (eds) Geología y recursos naturales de la plataforma continental Argentina. In: 13th Congreso Geológico Argentino No. 3th Congreso de Exploración de Hidrocarburos, Buenos Aires, Proceedings, vol 5, pp 73–93
- Malumián N, Olivero EB (2006) El Grupo Cabo Domingo, Tierra del Fuego: bioestratigrafía, paleoambientes y acontecimientos del Eoceno-Mioceno marino. Rev Asoc Geol Argent 61:139–160
- Martínez MA, Prámparo MB, Quattrocchio ME, Zavala CA (2008) Depositional environments and hydrocarbon potential of the Middle Jurassic Los Molles Formation, Neuquén Basin, Argentina: palynofacies and organic geochemical data. Rev Geol Chile 35(2):279–305
- Martínez MA, Olivera DE, Zavala C, Quattrocchio ME (2016) Palynotaphofacies analysis applied to Jurassic marine deposits, Neuquén Basin. Argent Facies 62(2):1–10
- McArthur AD, Kneller BC, Wakefield MI, Souza PA, Kuchle J (2016) Palynofacies classification of the depositional elements of confined turbidite systems: examples from the Gres d'Annot, SE France. Mar Pet Geol 77:1254–1273
- Mignard SLA, Mulder T, Martinez P, Charlier K, Rossignol L, Garlan T (2017) Deep-sea terrigenous organic carbon transfer and accumulation: impact of sea-level variations and sedimentation processes off the Ogooué River (Gabon). Mar Pet Geol 85:35–53
- Mulder T, Syvitski JPM, Migeon S, Faugères JC, Savoye B (2003) Marine hyperpycnal flows: initiation, behavior and related deposits. A review. Mar Pet Geol 20:861–882

- Oboh-Ikuenobe FE, de Villiers SE (2003) Dispersed organic matter in samples from the western continental shelf of Southern Africa: palynofacies assemblages and depositional environment of late Cretaceous and younger sediments. *Palaeogeogr Palaeoclimatol Palaeoecol* 201:67–88
- Olivero EB, Malumián N (2008) Mesozoic-Cenozoic stratigraphy of the Fuegian Andes, Argentina. *Geol Acta* 6:5–18
- Olivero EB, Martinioni DR (2001) A review of the geology of the Argentinean Fuegian Andes. *J S Am Earth Sci* 14:175–188
- Olivero EB, Malumián N, Palamarczuk S (2003) Estratigrafía del Cretácico superior-Paleógeno del área de bahía Thetis, Andes fueguinos Argentina acontecimientos biológicos y paleobiológicos. *Rev Geol Chile* 30:245–263
- Pacton M, Gorin GE, Vasconcelos C (2011) Amorphous organic matter—experimental data on formation and the role of microbes. *Rev Palaeobot Palynol* 166(3–4):253–267
- Parry CC, Whitley PKJ, Simpson RDH (1981) Integration of palynological and sedimentological methods in facies analysis of the Brent Formation. In: Illing LV, Hobson GD (eds) *Petroleum geology of the continental shelf of North West Europe*. Heyden, London, pp 205–215
- Plink-Björklund P, Steel R (2004) Initiation of turbidity currents: outcrop evidence for Eocene hyperpycnal flow turbidites. *Sediment Geol* 165:29–52
- Ponce JJ, Carmona NB (2011a) Coarse-grained sediment waves in hyperpycnal clinoform systems, Miocene of the Austral foreland basin. *Argent Geol* 39(8):763–766
- Ponce JJ, Carmona NB (2011b) Miocene deep-marine hyperpycnal channel-levee complexes, Tierra del Fuego, Argentina: facies associations and architectural elements. In: Slatt RM, Zavala C (eds) *Sediment transfer from shelf to deep water-revisiting the delivery system*, vol 6. American Association of Petroleum Geologists, Tulsa, pp 75–93
- Ponce JJ, Olivero ED, Martinioni DR (2008) Upper Oligocene-Miocene clinoforms of the foreland Austral Basin of Tierra del Fuego, Argentina: stratigraphy, depositional sequences and architecture of the foredeep deposits. *J S Am Earth Sci* 26(1):36–54
- Ramos VA, Haller MJ, Butrón F (1986) Geología y evolución tectónica de las Islas Barnevelt: atlántico Sur. *Rev Asoc Geol Argent* 40:137–154
- Ratan R, Chandra A (1983) Palynological investigations of the Arabian Sea sediments: fungal spores. *Geophytology* 13(2):195–201
- Robbiano JA, Arbe H, Gangui A (1996) Cuenca Austral marina. In: Ramos VA, Tunic MA (eds) *Geología y recursos naturales de la plataforma continental argentina*. In: 13th Congreso Geológico Argentino No, 3th Congreso de Exploración de Hidrocarburos, Buenos Aires, Proceedings, vol 17, pp 323–341
- Slater SM, McKie T, Vieira M, Wellman CH, Vajda V (2017) Episodic river flooding events revealed by palynological assemblages in Jurassic deposits of the Brent Group, North Sea. *Palaeogeogr Palaeoclimatol Palaeoecol* 485:389–400
- Stetten E, Baudin F, Reyss JL, Martinez P, Charlier K, Schnyder J, Rabouille C, Dennielou B, Coston-Guarini J, Pruski AM (2015) Organic matter characterization and distribution in sediments of the terminal lobes of the Congo deep-sea fan: evidence for the direct influence of the Congo River. *Mar Geol* 369:182–195
- Tyson RV (1995) *Sedimentary organic matter*. Chapman and Hall, London
- Tyson RV, Follows B (2000) Palynofacies prediction of distance from sediment source: a case study from the Upper Cretaceous of the Pyrenees. *Geology* 28(6):569–571
- Volkheimer W, Melendi DL (1976) Palinomorfos como fósiles guía (3ra. parte). *Técnicas del laboratorio palinológico*. *Rev Min de Geol y Min* 34:19–30
- Zavala C, Arcuri M (2016) Intrabasinal and extrabasinal turbidites: origin and distinctive characteristics. *Sediment Geol* 337:36–54
- Zavala C, Gamero H, Arcuri M (2006) Lofting rhythmmites: a diagnostic feature for the recognition of hyperpycnal deposits. In: 2006 GSA Annual Meeting, Philadelphia, Proceedings, pp 22–25
- Zavala C, Arcuri M, Blanco Valiente L (2012) The importance of plant remains as diagnostic criteria for the recognition of ancient hyperpycnites. *Revue de Paléobiologie Genève Vol Spéc* 11:457–469